

Solar coronal lines in the visible and infrared. DKIST

Giulio Del Zanna

DAMTP, University of Cambridge (UK)



Forbidden lines in the visible/IR are great to measure

- Ne via line ratios or actual radiances
- Te (ionisation T, but also Te in combination with EUV)
- Chemical abundances
- Non-Thermal effects (line widths, non-thermal electrons)
- Magnetic field

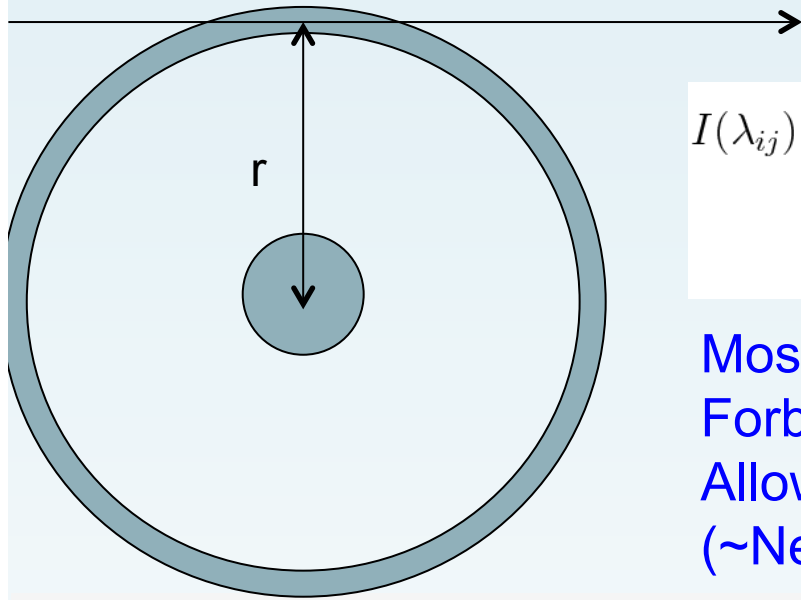
However: atomic data modelling and source modelling is not simple.

Del Zanna & Mason, 2018, Liv. Rev. Sol. Phys.

For a list of forbidden lines: Del Zanna & DeLuca (2017)

Modelling the outer corona: Del Zanna+2018 (soon in ArXiv)

For details on CHIANTI modelling: user guide



$$I(\lambda_{ij}) = \frac{h\nu_{ij}}{4\pi} \int N_j A_{ji} dh = \int Ab(X)C(T, \lambda_{ij}, N_e)N_eN_H dh \quad [\text{ergs}$$

$$C(T, \lambda_{ij}, N_e) = \frac{h\nu_{ij}}{4\pi} \frac{A_{ji}}{N_e} \frac{N_j(X^{+m})}{N(X^{+m})} \frac{N(X^{+m})}{N(X)}$$

Most allowed (EUV) transitions: $C(T)$; $I \sim N_e^2$

Forbidden: $C(T, N_e, r, I_{\text{disk}})$

Allowed, forbidden and scattered I_{disk} emission ($\sim N_e$) is not necessarily co-spatial

Si X 1.43 microns contribution function

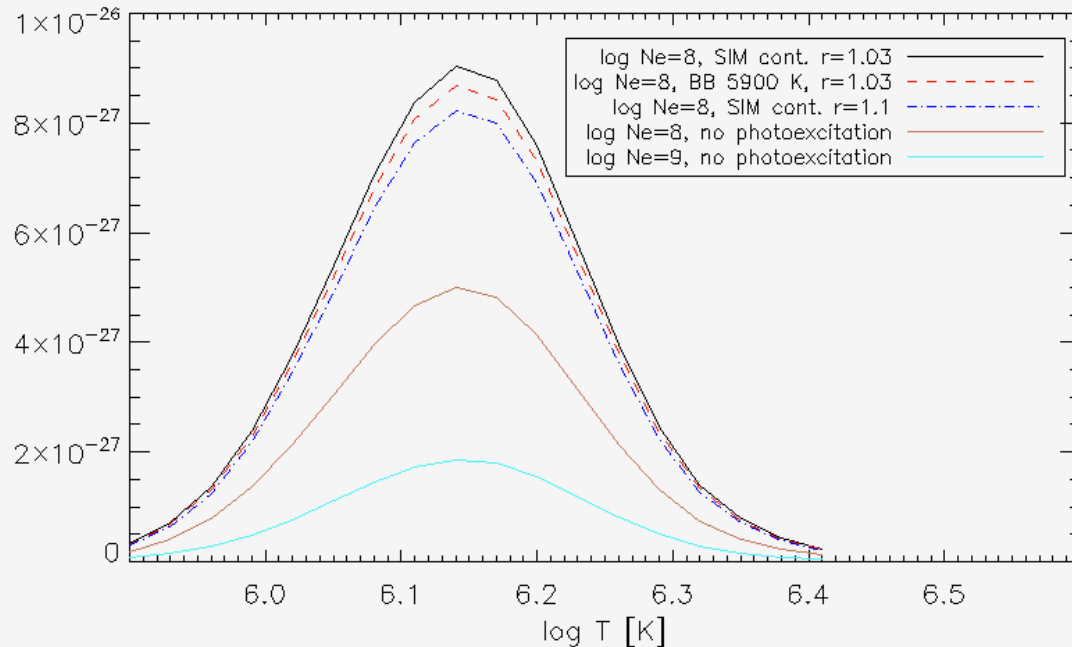
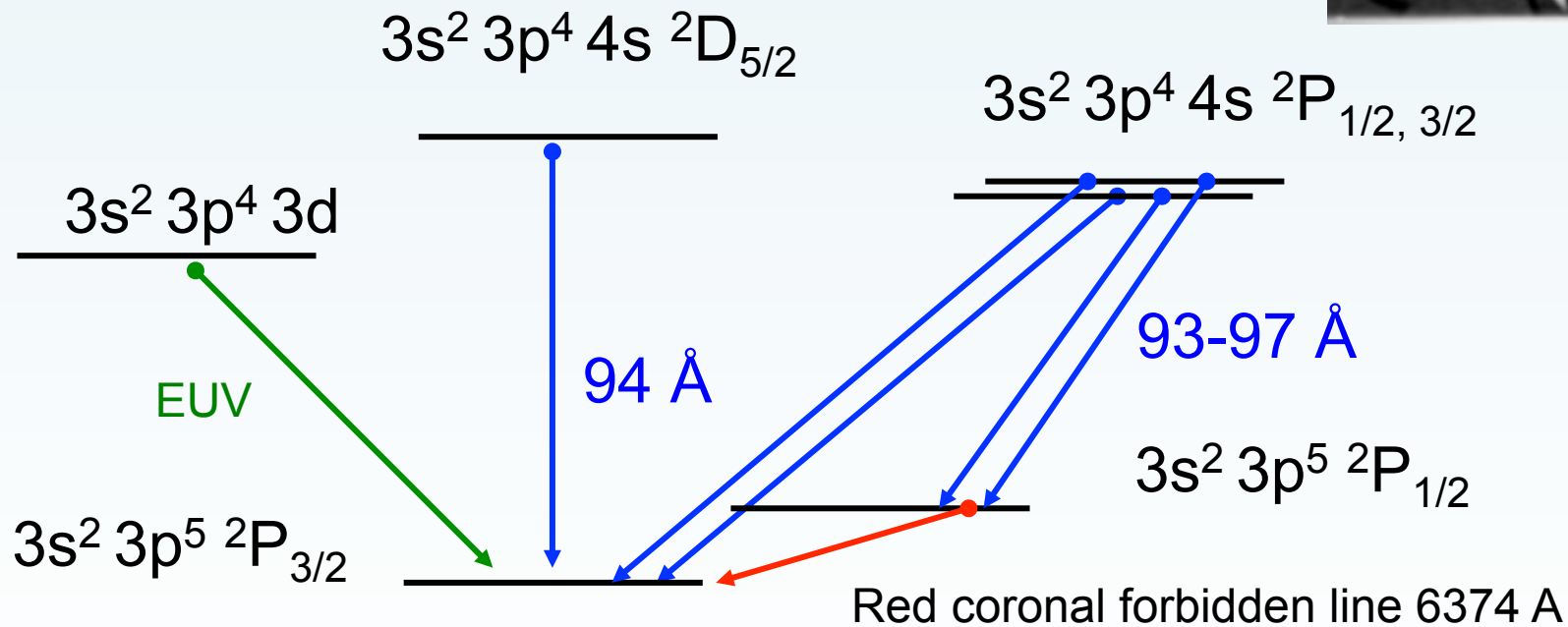


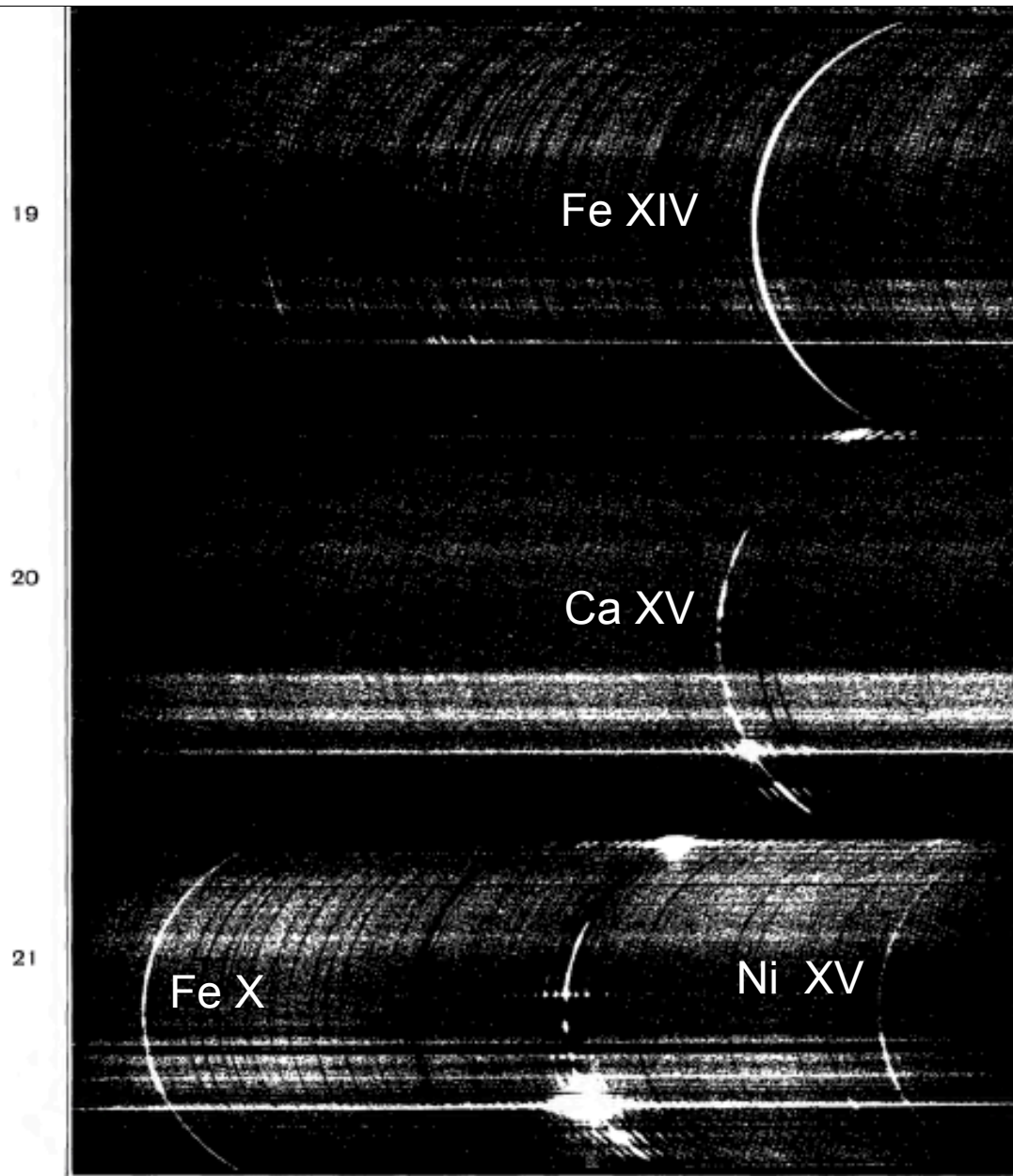
Photo-excitation from disk is significant, but can be modelled using CHIANTI, with user-defined disk radiances. Disk profiles and local absorption can be tricky (Doppler dimming) but for DKIST lines should be a minor issue.

The forbidden lines

Known thanks to Fe X identifications in the soft X-rays from Edlen in 1930's.

Side note: significant updates in the soft X-rays are Fawcett (1972) and Del Zanna (2012), but a lot more is still needed.





Spectra of the corona and prominences.

Fig. 18.—Line $\lambda 3388$.

Fig. 19.—Lines $\lambda\lambda 5116$ and 5303 .

Fig. 20.—Lines $\lambda 5694$ and D_2 .

Fig. 21.—Lines $\lambda 6374$, $H\alpha$, and $\lambda 6702$.

Bernard Lyot, George Darwin Lecture.

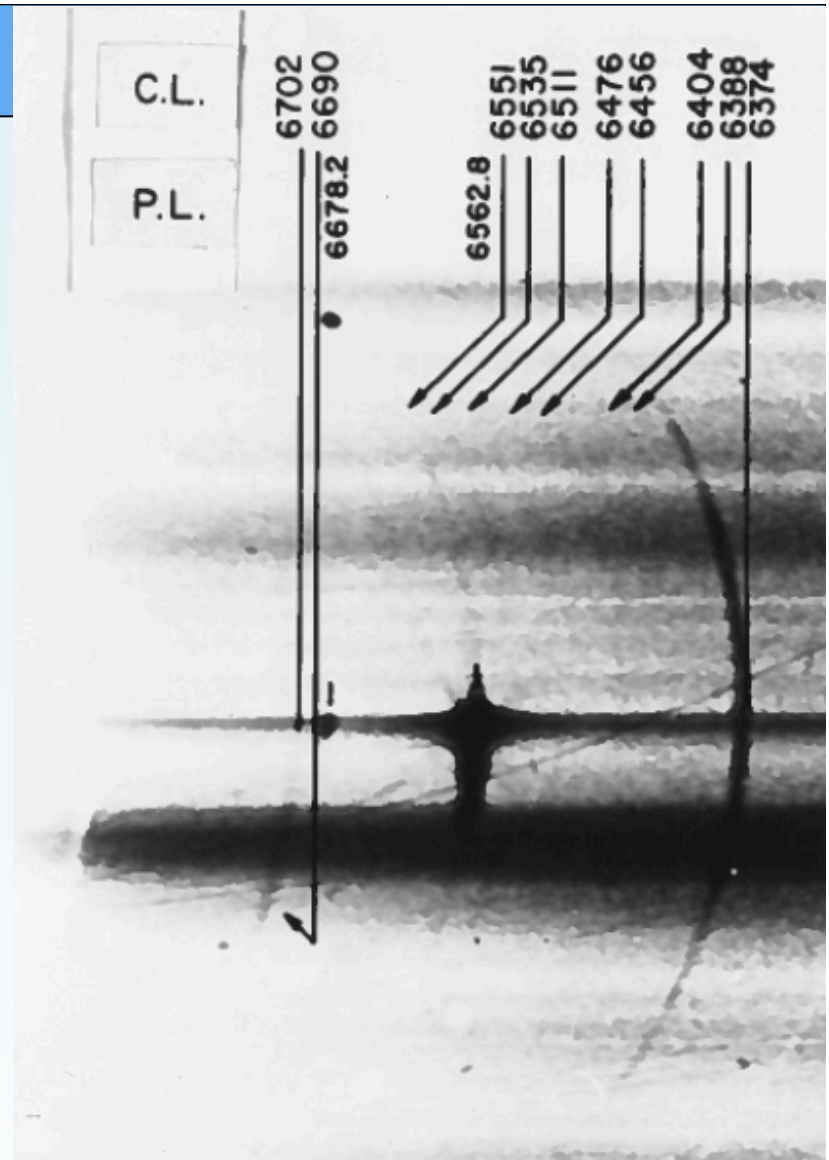


Lyot (1939): breakthrough measurements of 11 coronal lines in the visible and near-infrared at Pic du Midi, outside eclipses.

Lyot's 1952 observation

Lyot obtained what are still the best observations of coronal lines from near-UV to near-infrared during an eclipse in 1952.

He died after 3 months, still in Egypt.



VISIBLE SPECTRUM OF THE INNER CORONA OBTAINED DURING THE TOTAL ECLIPSE OF 1952 FEBRUARY 25 AT KHARTOUM BY ALY AND LYOT. WEST LIMB

Atomic data



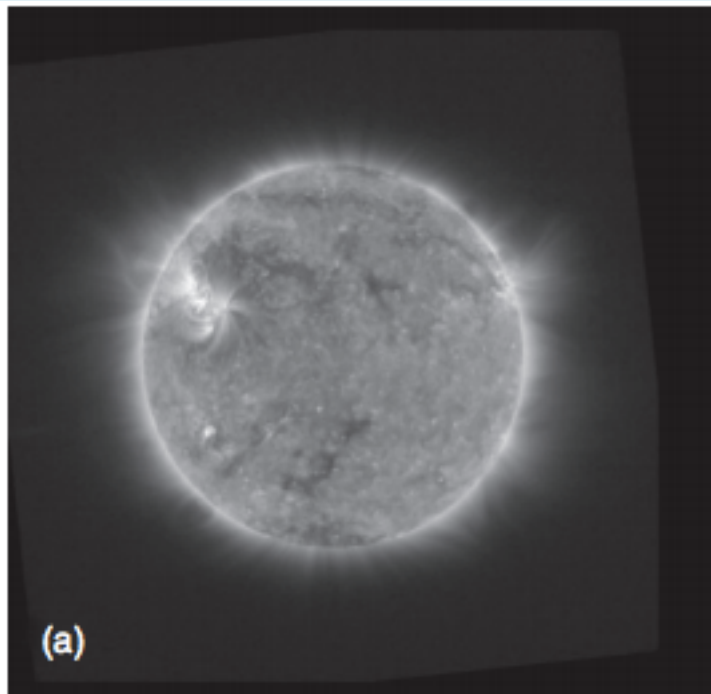
Seaton and Eissner wrote a code in the early 1970's at UCL for the calculation of electron-ion cross-sections.

Seaton's PhD student (Helen Mason) was tasked to carry out the first calculations for the iron coronal ions (Mason 1975a).

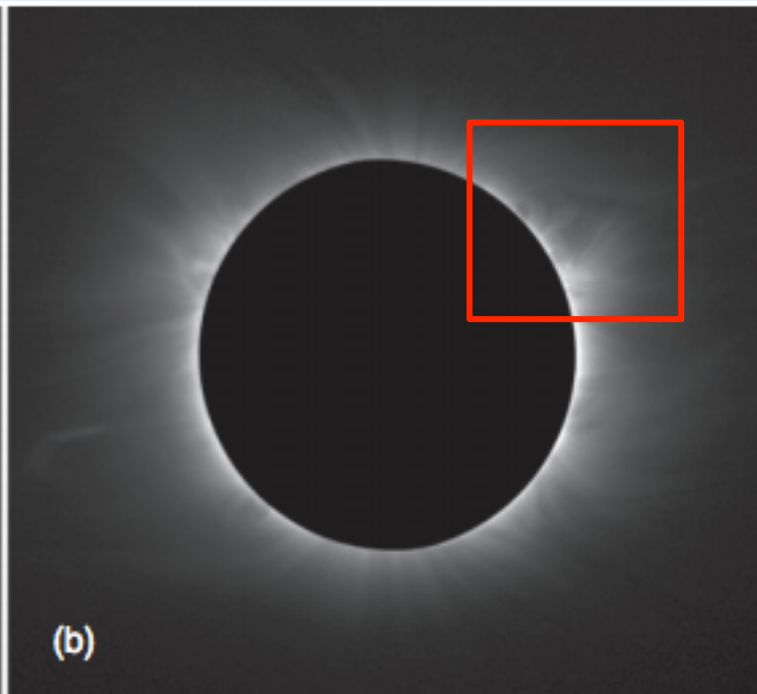
Seaton and Burgess also provided ionization and recombination.

With major contributions from Burgess, Burke (Belfast), Berrington, the Iron Project work in the 80's and 90's. These codes are still used today.

Why bother with the forbidden lines?



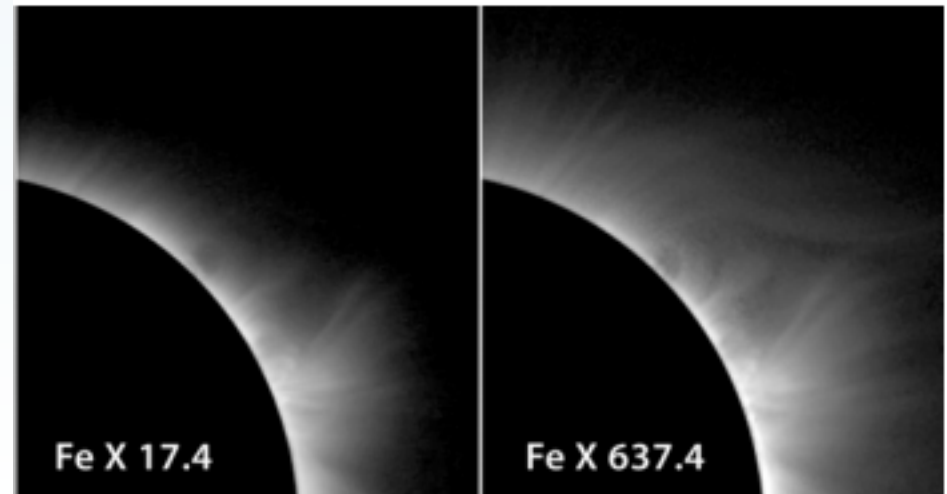
EUV



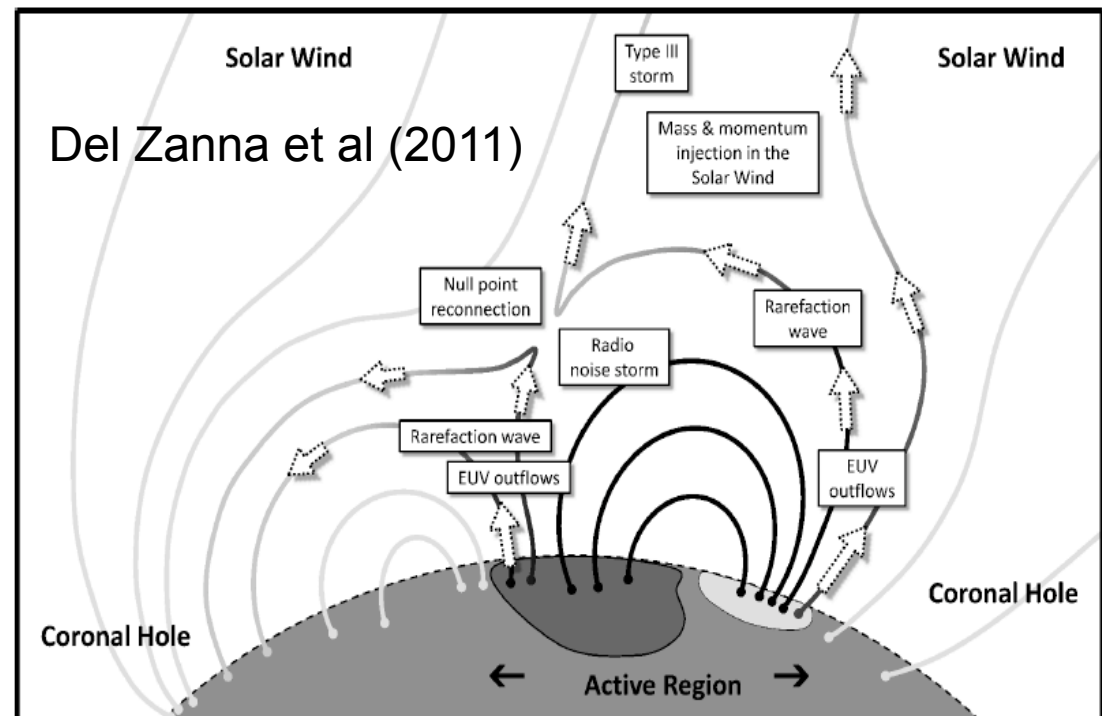
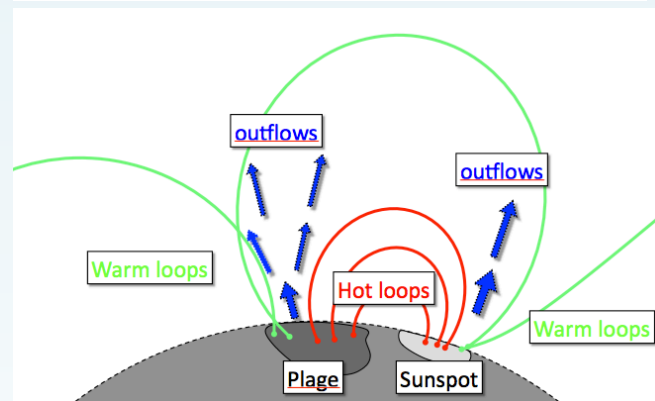
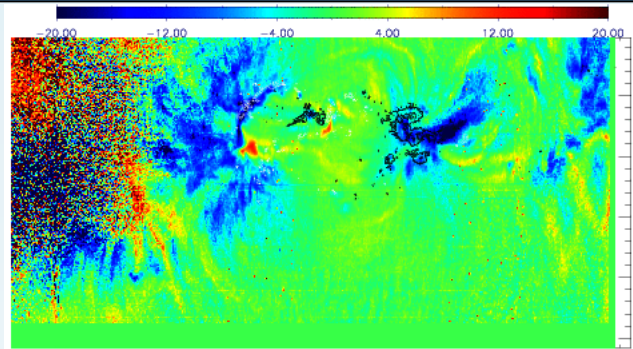
VISIBLE

Habbal+(2011)

Forbidden lines in the visible/near infrared are partly photoexcited from the photospheric radiation, hence are visible at greater distances, where many unknown processes occur: acceleration of the solar wind and CME, reconnection



Interchange reconnection at 1 R_{sun}

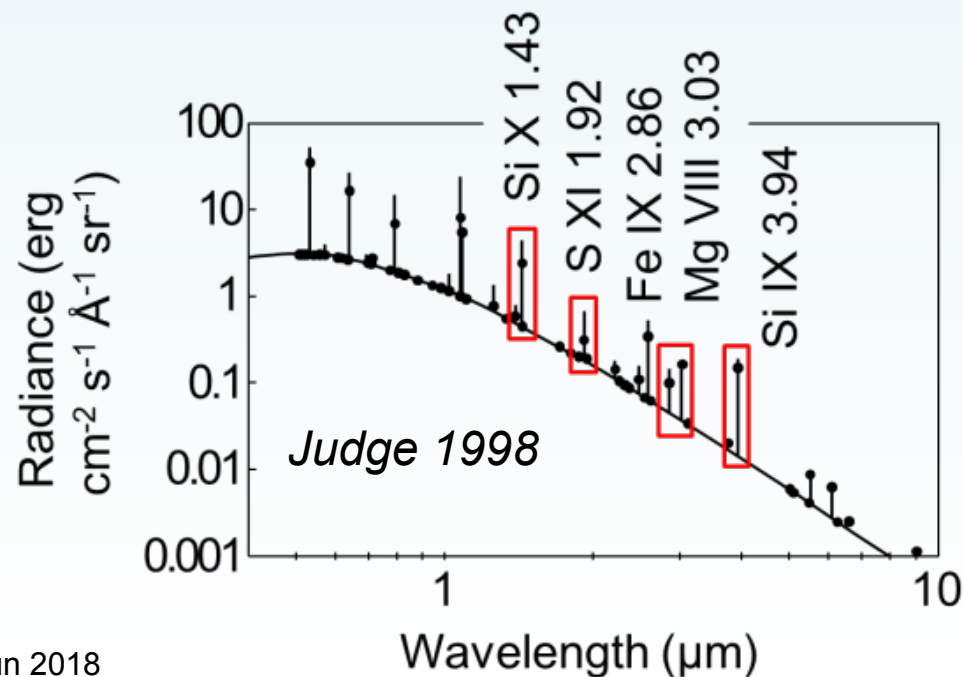


(Del Zanna+2011): interchange reconnection close to the null point, coronal upflows (Del Zanna 2008) driven by a rarefaction wave (Bradshaw, Aulanier & Del Zanna, 2011). [Solar Orbiter and DKIST can provide important clues.](#)

[Most of the Solar Orbiter encounters will be in near quadrature, i.e. excellent synergy with DKIST, which in principle can measure the FIP in 1-4 MK plasma \(see below\).](#)

Judge (1998) predicted line radiances (mostly in the IR) using

- 1) CHIANTI v.1 (1997)
- 2) constant T distribution 0.8-3 MK
- 3) 'Coronal' abundances, i.e 4x photospheric.
- 4) black body disk spectrum at 5900 K



Forbidden visible/IR lines

SOLAR CORONAL LINES IN THE VISIBLE AND INFRARED. A ROUGH GUIDE

GIULIO DEL ZANNA

DAMTP, CMS, University of Cambridge, Wilberforce Road, Cambridge CB3 0WA, United Kingdom

EDWARD E. DELUCA

Harvard-Smithsonian Center for Astrophysics, 60 Garden Street, Cambridge, MA 02138, United States

Draft version November 22, 2017

Prompted by DKIST and AIR-Spec

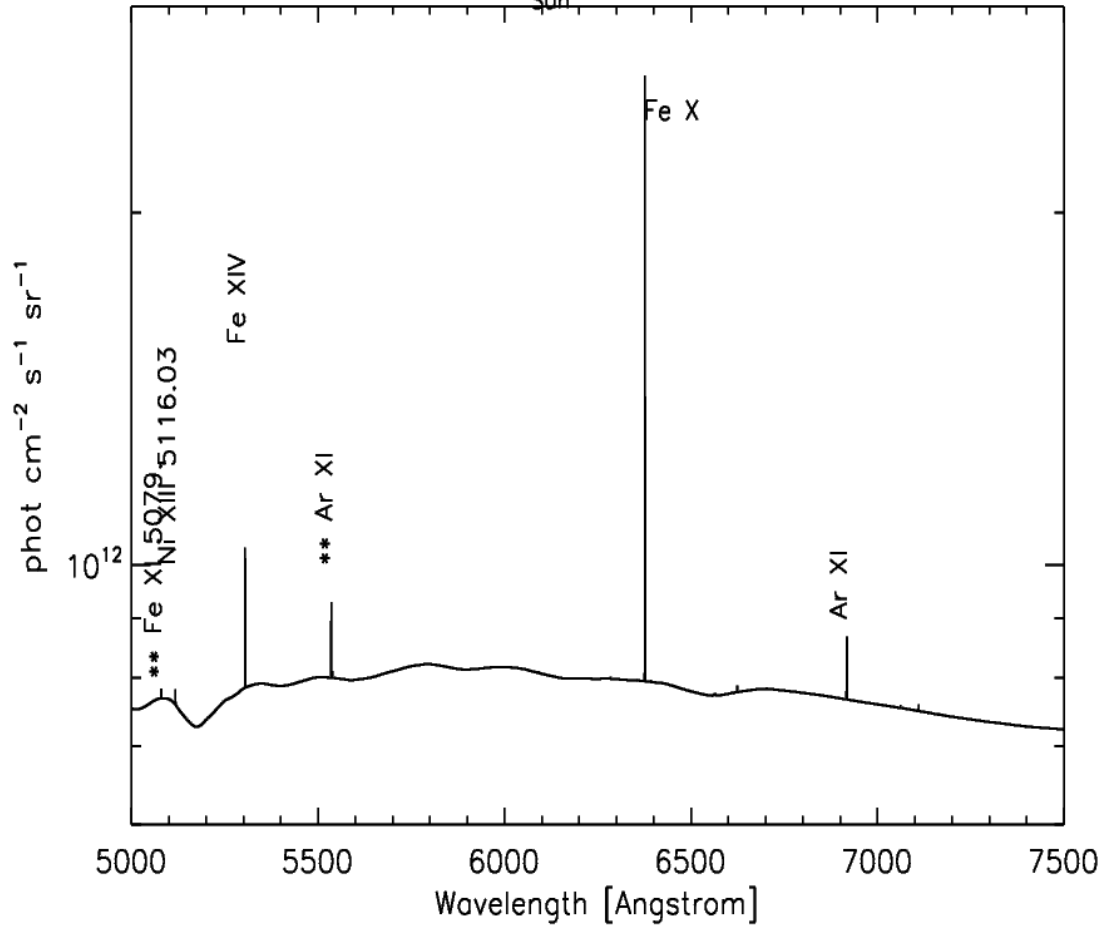
- Found in the literature large discrepancies in wavelengths (3 Å), identifications and intensities
- Predicted line intensities using the most recent atomic data and observations. Significant differences with Judge (1998) in some cases, due to:
 - 1) CHIANTI v.8
 - 2) Isothermal atmosphere;
 - 3) Photospheric abundances
- Confirm previous identifications on the basis of line intensities – NEW –
- Identify lines useful for diagnostics for DKIST – NEW

The visible and especially the IR are relatively unexplored !

Observed CHIANTI

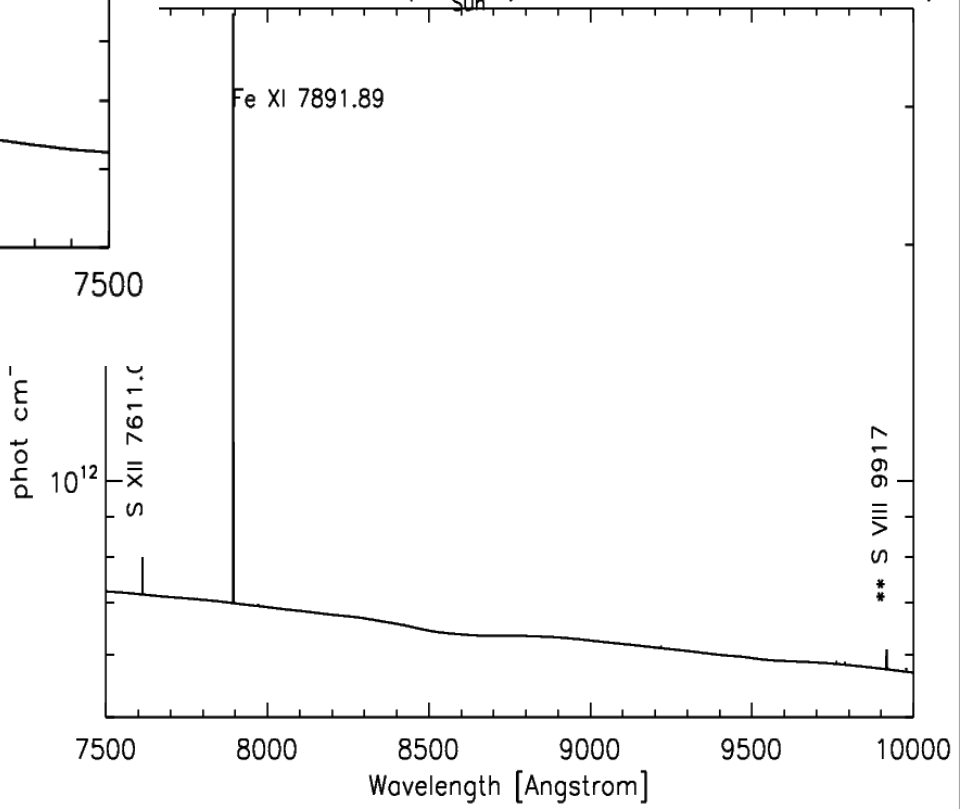
$\lambda_o(\text{air})$	$\lambda_o(\text{vac})$	λ_C	I(AR)	I(QR)	I(QS)	Ion	Notes	Transition
6374.56 ^{WF} (A)	6376.32	6376.3	163 (310, 280)	211 (200)	73 (57)	Fe X	J98:99	$3s^2 3p^5 \ ^2P_{3/2} - 3s^2 3p^5 \ ^2P_{1/2}$
? 6622.99 ^{WF}	6624.82	6624.3	(1.7)	(0.7)	(0.3)	? Fe XI	-	$3s^2 3p^3 3d \ ^3D_3 - 3s^2 3p^3 3d \ ^3F_4$
		? 6672.5	(2.4, 1.9)	-	-	K XIV	-	$2s^2 2p^2 \ ^3P_1 - 2s^2 2p^2 \ ^3P_2$
6701.47 ^{WF} (A)	6703.32	6703.5	216 (140, 99)	(0.5)	(0.03)	Ni XV	S77	$3s^2 3p^2 \ ^3P_0 - 3s^2 3p^2 \ ^3P_1$
6917.0 ^{WF}	6918.91	6918.0	(18, 8)	4 (6.6)	(3)	Ar XI	S77, J98:3.2	$2s^2 2p^4 \ ^3P_2 - 2s^2 2p^4 \ ^3P_1$
7059.59 ^{WF}	7061.54	7062.1	(200)	(1.1)	(0.08)	Fe XV	J98:3.5	$3s 3p \ ^3P_1 - 3s 3p \ ^3P_2$
		7548.3	(13, 4)	-	-	K XIV	-	$2s^2 2p^2 \ ^3P_0 - 2s^2 2p^2 \ ^3P_1$
7611.0 (II)	7613.1	7613.1	(260, 180)	23 (14)	3.4 (2.7)	S XII	S77	$2s^2 2p \ ^2P_{1/2} - 2s^2 2p \ ^2P_{3/2}$
7891.89 ^{WF}	7894.06	7894.0	(340, 290)	177 (420)	66 (93)	Fe XI	J98:85	$3s^2 3p^4 \ ^3P_2 - 3s^2 3p^4 \ ^3P_1$
8024.2 ^L (1)	8026.3	8026.3	(57)	(6×10^{-2})	-	Ni XV	-	$3s^2 3p^2 \ ^3P_1 - 3s^2 3p^2 \ ^3P_2$
		8339.6	(20)	-	-	Ar XIII	J98:0.5	$2s^2 2p^2 \ ^3P_1 - 2s^2 2p^2 \ ^3P_2$
		9219.	(0.5)	(0.1)	-	Cl X	-	$2s^2 2p^4 \ ^3P_2 - 2s^2 2p^4 \ ^3P_1$
		9917	(8.5)	(4)	(1.5)	S VIII	J98:1.2	$2s^2 2p^5 \ ^2P_{3/2} - 2s^2 2p^5 \ ^2P_{1/2}$
		9919	(4.3)	(0.5)	(0.1)	Fe XIII	-	$3s^2 3p 3d \ ^3F_3 - 3s^2 3p 3d \ ^3F_4$
		9978	(1.1)	(0.4)	(0.2)	Mn X	-	$3s^2 3p^4 \ ^3P_2 - 3s^2 3p^4 \ ^3P_1$
		10143	(38)	-	-	Ar XIII	J98:8	$2s^2 2p^2 \ ^3P_0 - 2s^2 2p^2 \ ^3P_1$
		10301	(13)	-	-	S XIII	-	$2s 2p \ ^3P_1 - 2s 2p \ ^3P_2$
		10651	(2)	-	-	Cl XII	-	$2s^2 2p^2 \ ^3P_1 - 2s^2 2p^2 \ ^3P_2$
10746.80 ^L (15)	10749.7	10749.	(4.3×10^2)	(240)	(35)	Fe XIII	J98:285	$3s^2 3p^2 \ ^3P_0 - 3s^2 3p^2 \ ^3P_1$
10797.95 ^L (15)	10801.	10801.	(3.4×10^2)	(140)	(21)	Fe XIII	J98:67	$3s^2 3p^2 \ ^3P_1 - 3s^2 3p^2 \ ^3P_2$
	12660	? 12524	224 ^O (14)	(4.7)	(4.7)	S IX	J98:13 (not Fe XIV)	$2s^2 2p^4 \ ^3P_2 - 2s^2 2p^4 \ ^3P_1$
		12793	(2.7)	-	-	Ni XIV	-	$3s^2 3p^3 \ ^2D_{3/2} - 3s^2 3p^3 \ ^2D_{5/2}$
		13837	(4)	-	-	Cl XII	-	$2s^2 2p^2 \ ^3P_0 - 2s^2 2p^2 \ ^3P_1$
		13928	(50)	(7)	(3.5)	S XI	J98:6	$2s^2 2p^2 \ ^3P_1 - 2s^2 2p^2 \ ^3P_2$

QS off-limb at 1.1 R/R_{Sun} (Del Zanna & DeLuca 2017)

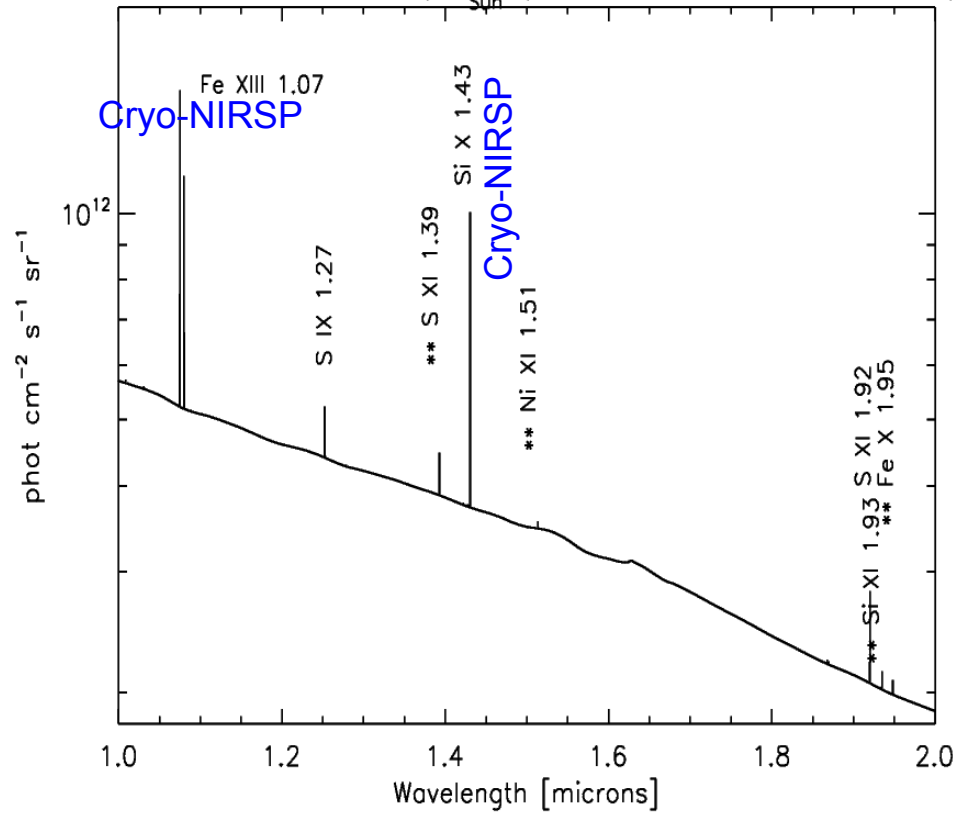


K-corona is a recent calculation

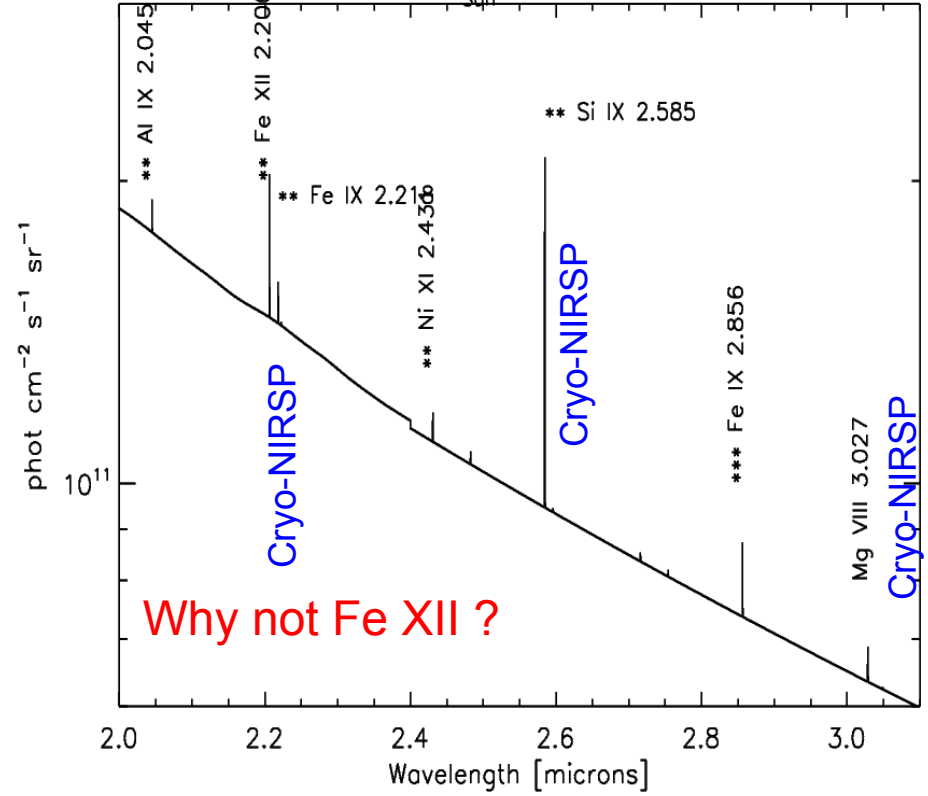
QS off-limb at 1.1 R/R_{Sun} (Del Zanna & DeLuca 2017)



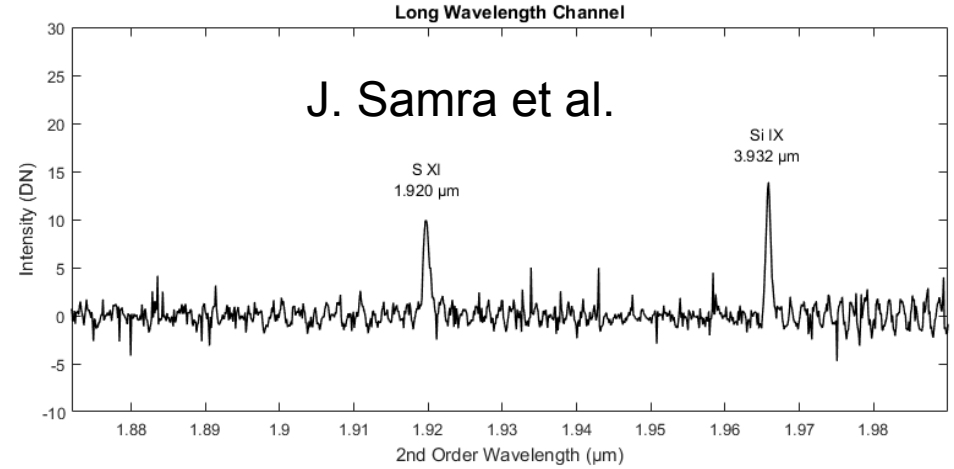
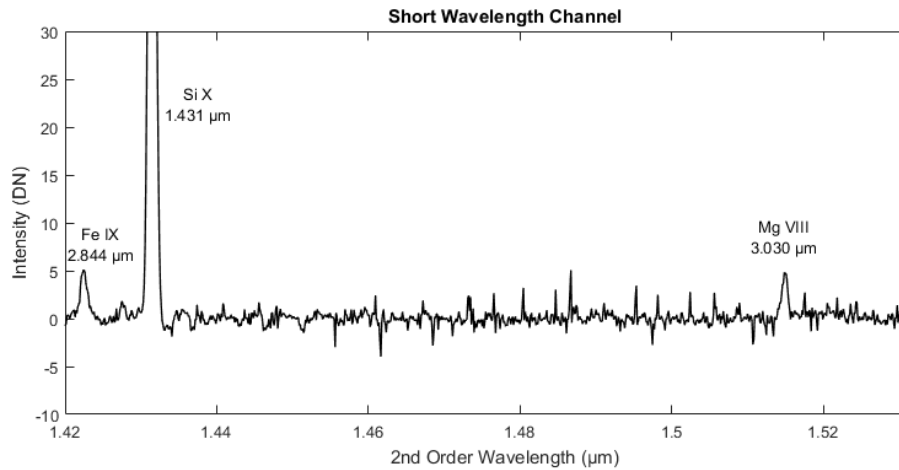
QS off-limb at 1.1 R/R_{Sun} (Del Zanna & DeLuca 2017)



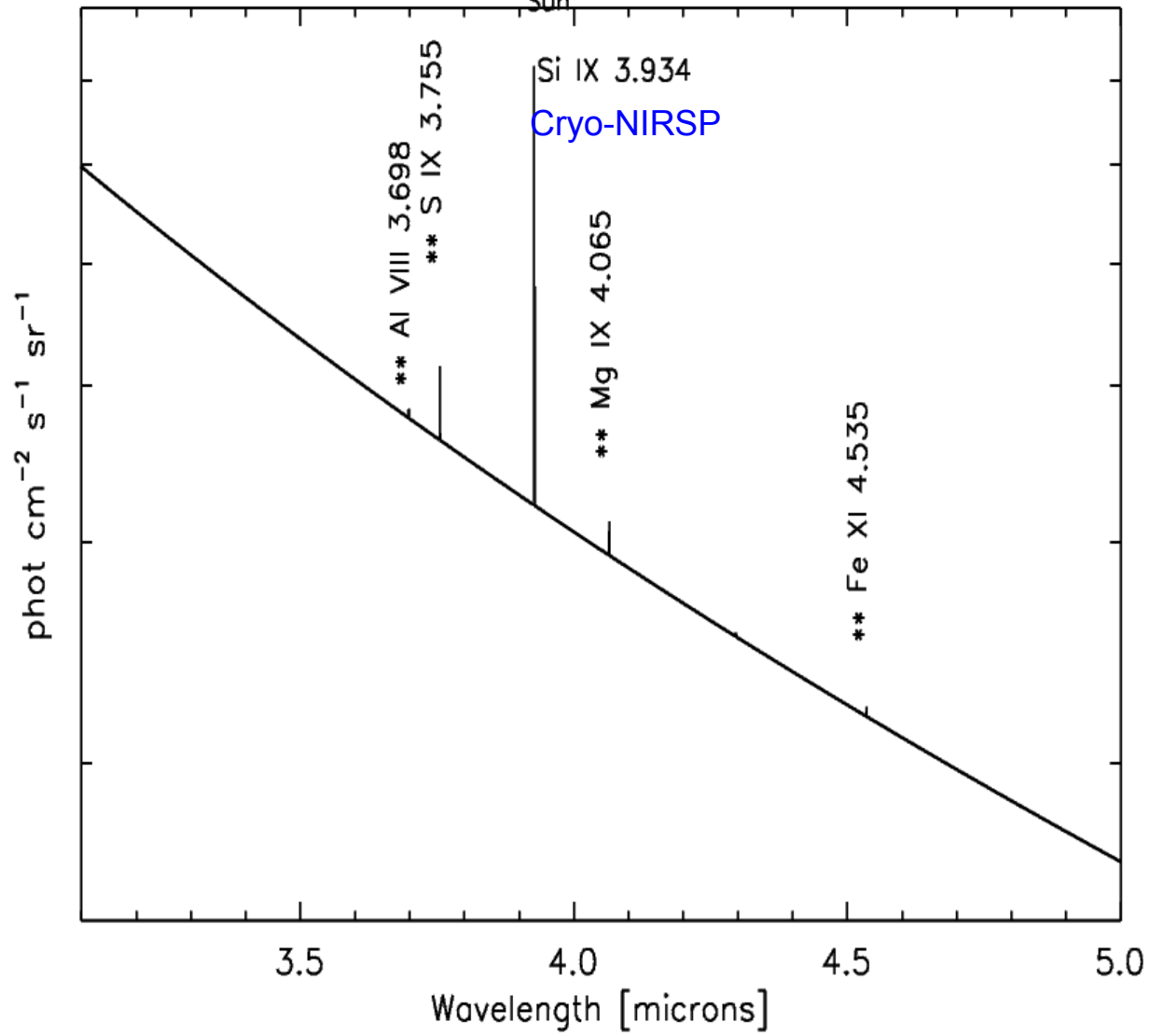
QS off-limb at 1.1 R/R_{Sun} (Del Zanna & DeLuca 2017)



Airspec – IR spectra during total eclipse 2017

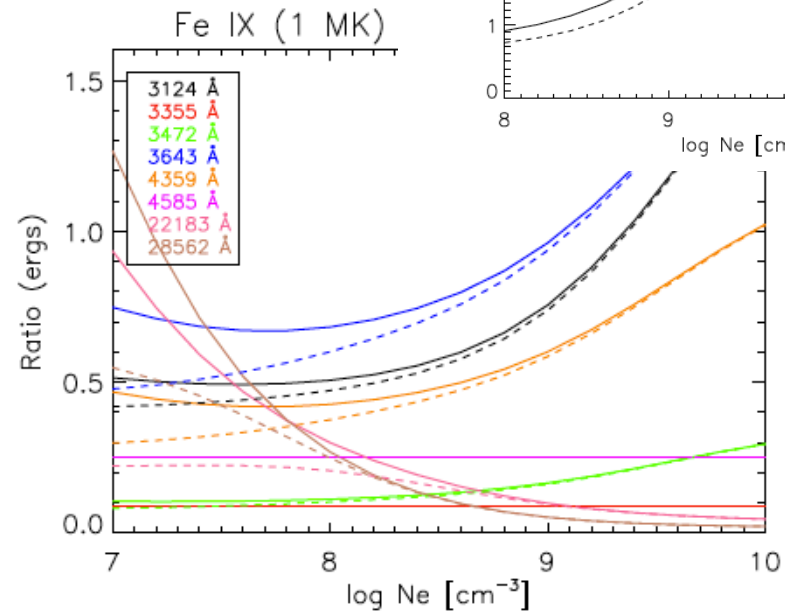
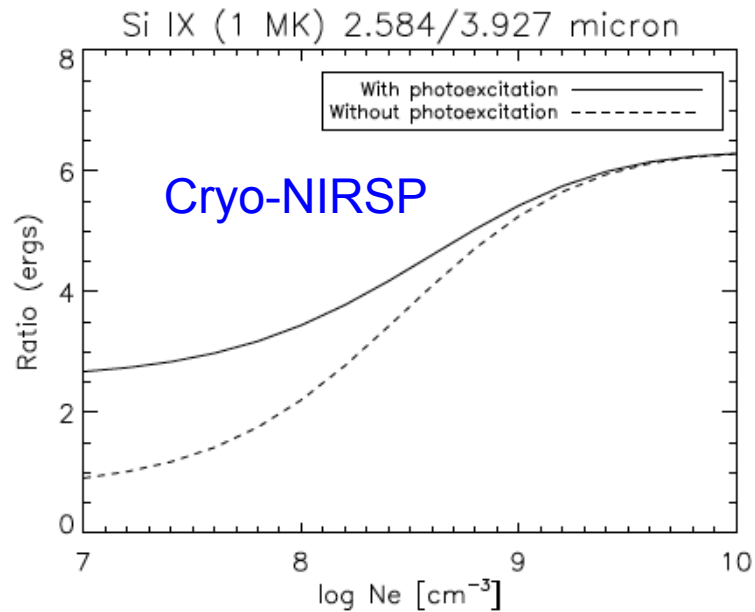
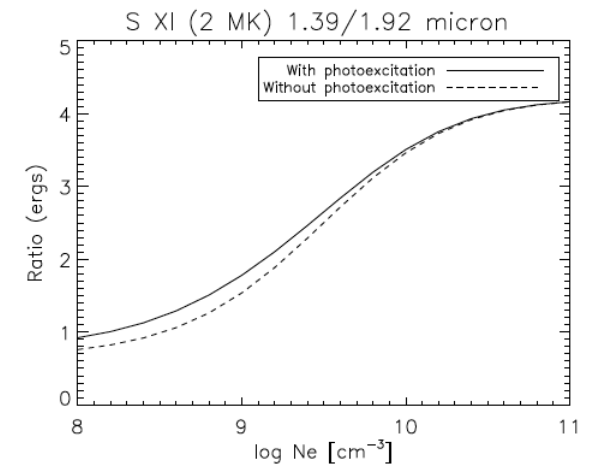
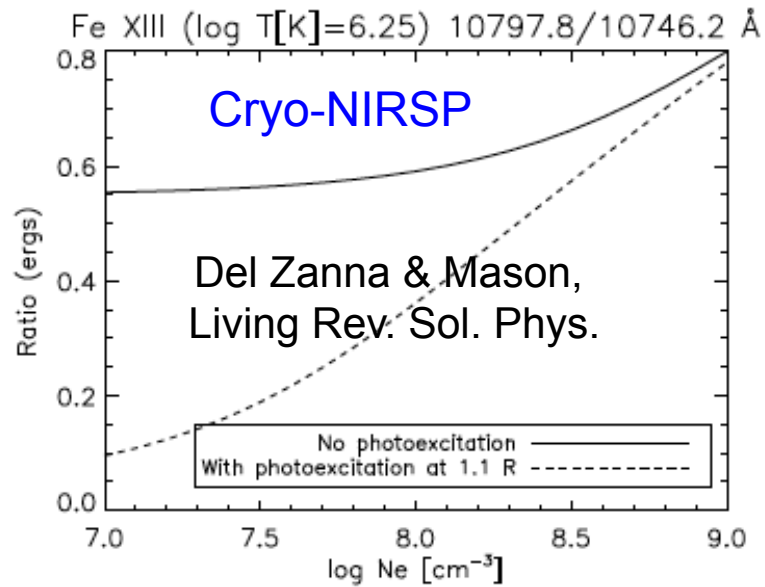


QS off-limb at 1.1 R/R_{Sun} (Del Zanna & DeLuca 2017)

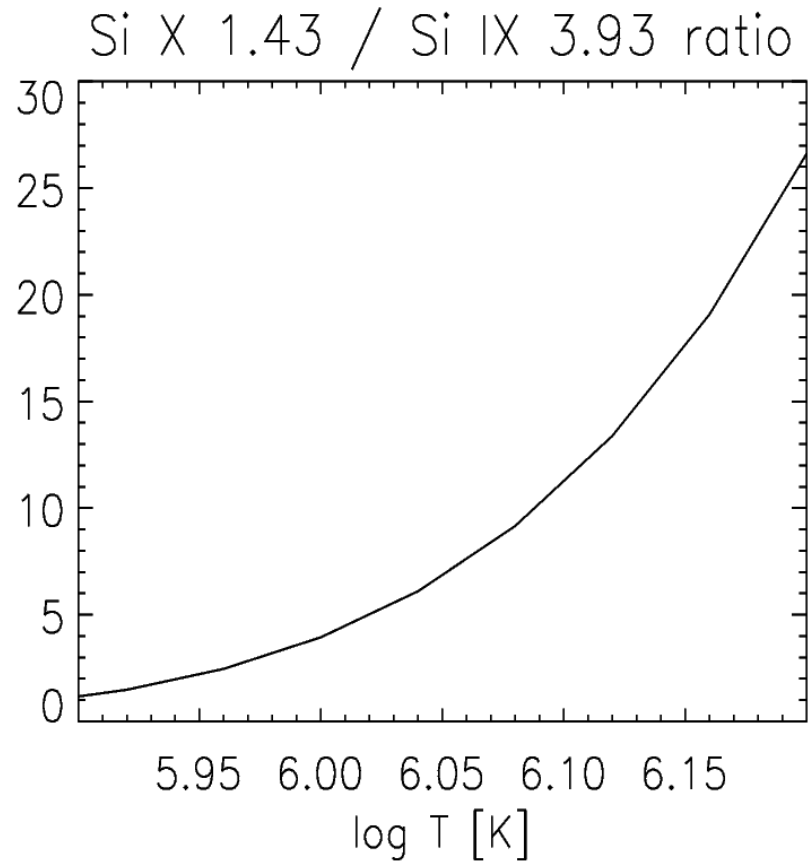
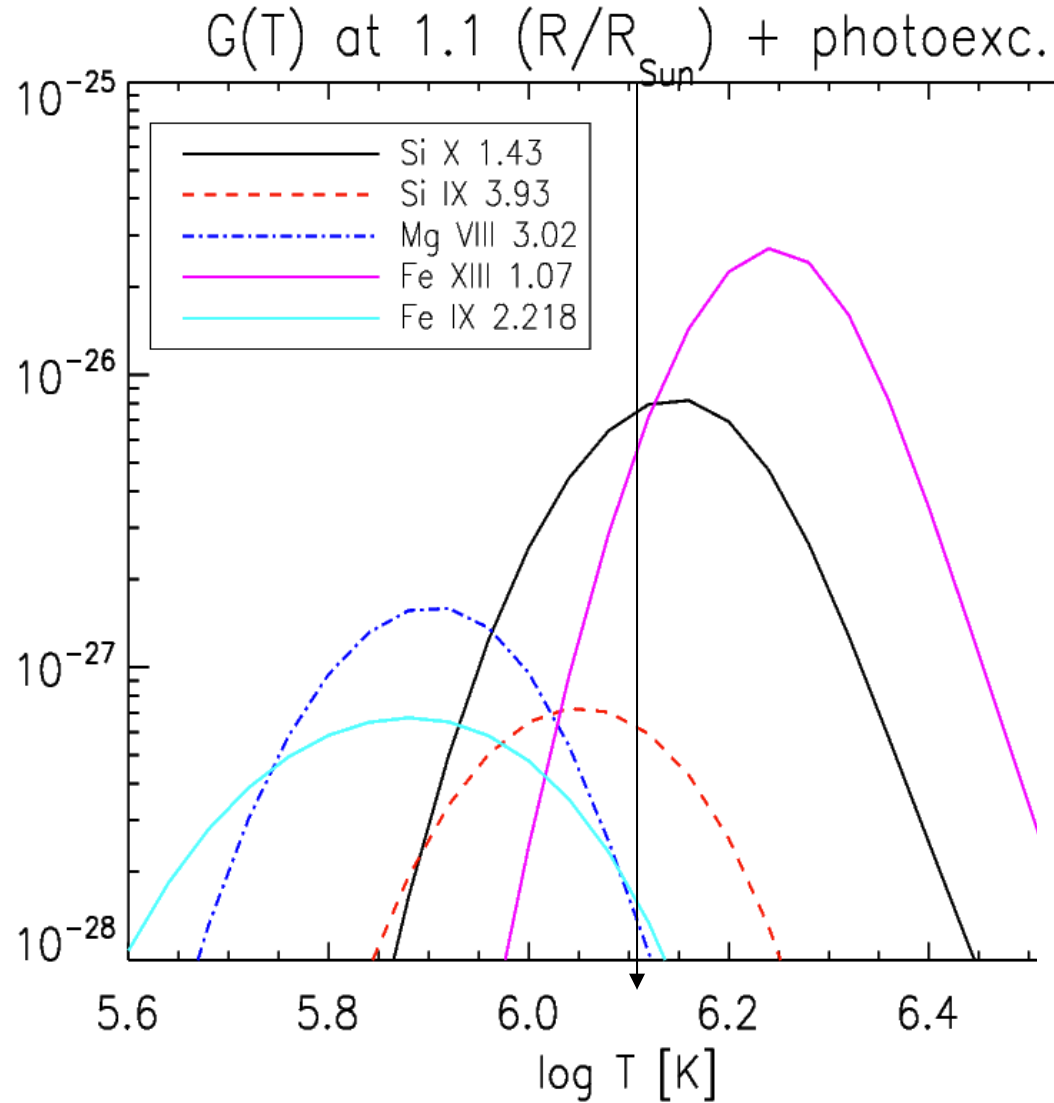


Measurements of Ne

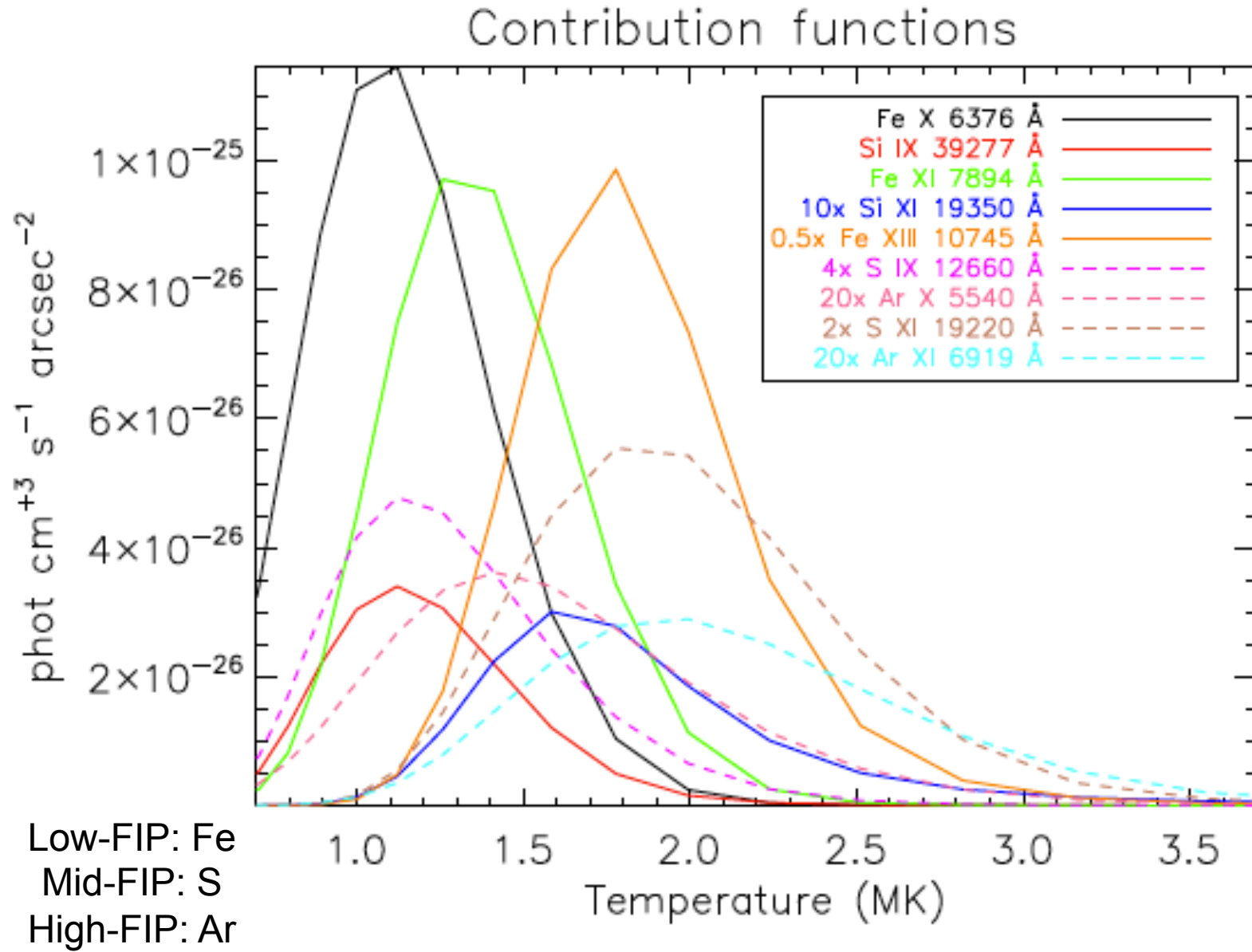
Ion	λ_1 (Å)	λ_2 (Å)	T (MK)	$\log N_e$ (cm^{-3})
Fe IX	3124	3355	1	8.5–11
Fe IX	3644	3802	1	8–11
Fe IX	4360	4588	1	8–11
Fe IX	22183	28563	1	7–9.5
Fe X	6376	3454	1	9–11
Fe X	3021	3454	1	9–11
Fe XI	3988	7894	1.5	9–11
Si IX	25846	39277	1	8–9
S XI	13928	19220	2	8–10
Fe XIII	10801	10749	2	7–11
Ar XIII	8339	10143	3	9.5–11.5
Ca XV	5446	5696	4.5	8–10.5



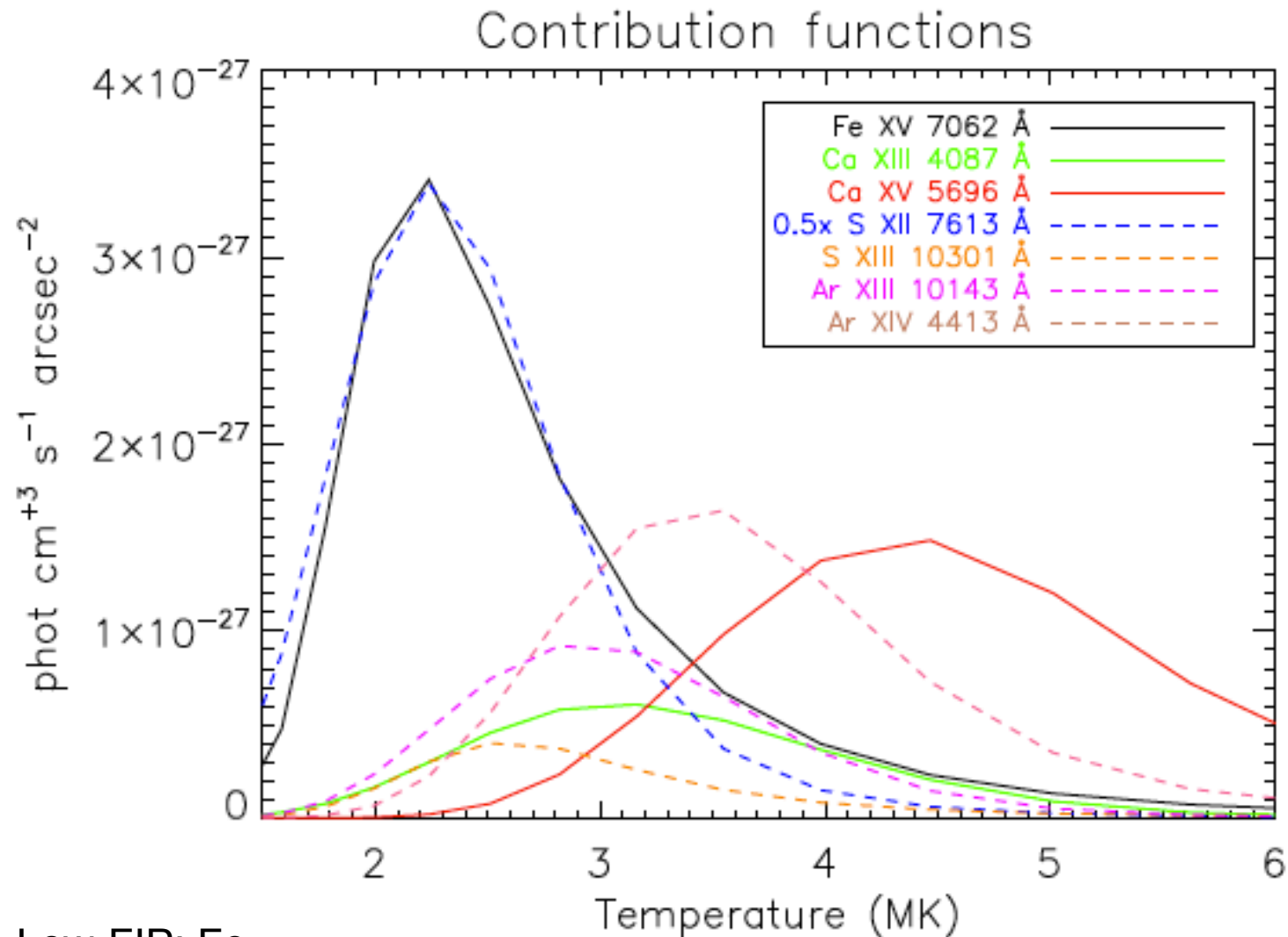
Lines in the current selection – ionisation T



Potential lines for abundance measurements (1)



Potential lines for abundance measurements (2)



Low-FIP: Fe
Mid-FIP: S
High-FIP: Ar

For AR core loops best lines are Ar XIII and Ca XIII (or Ni XV, seen by Lyot)

Issues on atomic data for the forbidden lines

The electron collisional data are still not well known or missing for many ions.

Significant improvement in CHIANTI v.8 (Del Zanna+2015) for the iron ions (Del Zanna, several). Factors of ~ 2 differences in intensities !
Be-like and Mg-like will be available in CHIANTI v.10

Main provider: **UK APAP Network**: <http://www.apap-network.org/>

STFC (UK) funding available to calculate C-,N-,O-like ions

- Fe IX OK.
- Si IX C-like not so good.
- Si X UK APAP OK
- Mg VIII UK APAP data OK
- S XI C-like not so good.

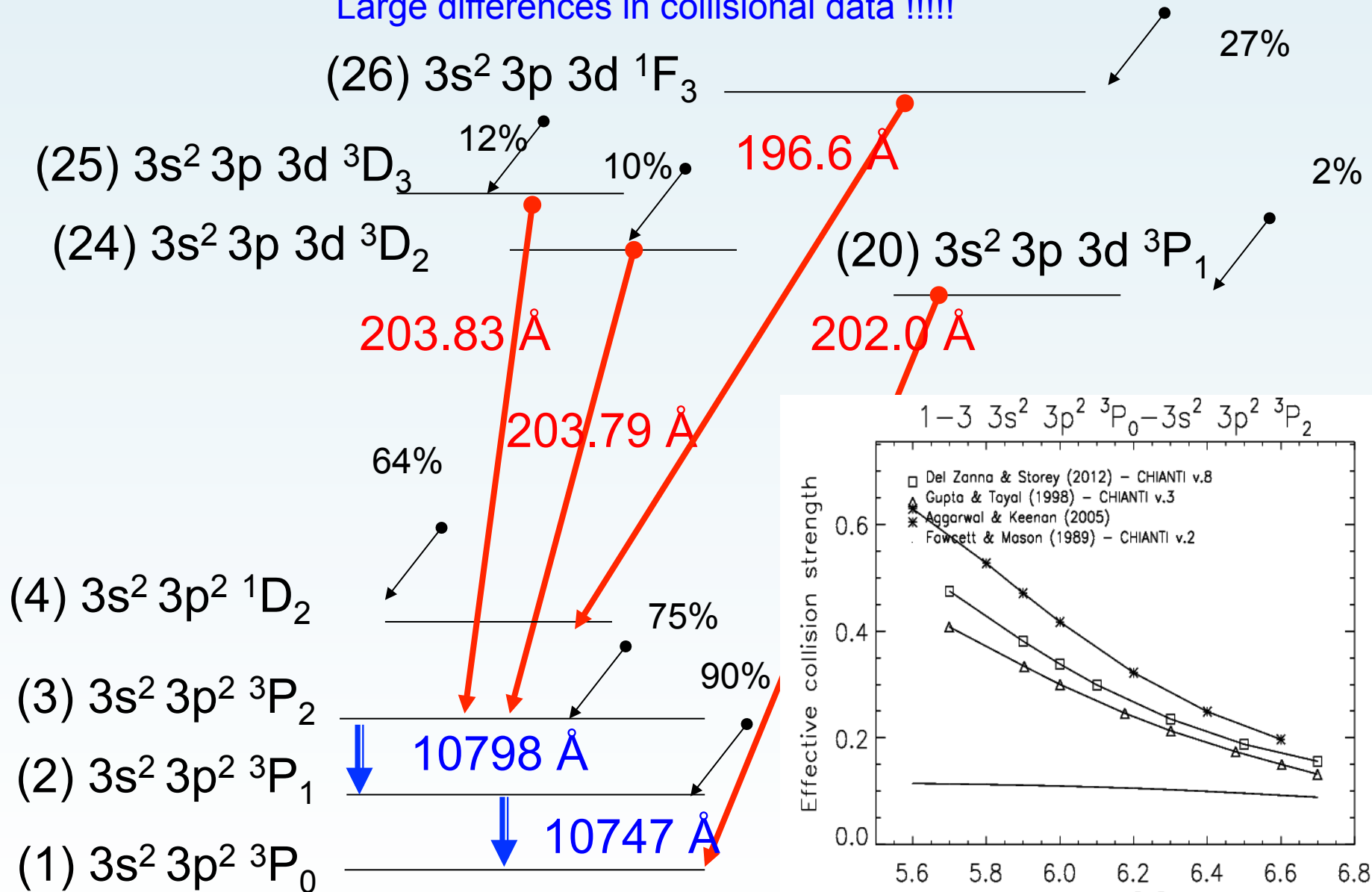
Rest wavelengths need improvements.

**Community support for laboratory astrophysics is needed
(support IAU symposium in Cambridge UK, Apr 2019 !)**



Fe XIII – log Ne=8

Complex cascading effects (Yu, Del Zanna+2018; Del Zanna & Mason 2018).
 Large differences in collisional data !!!!!

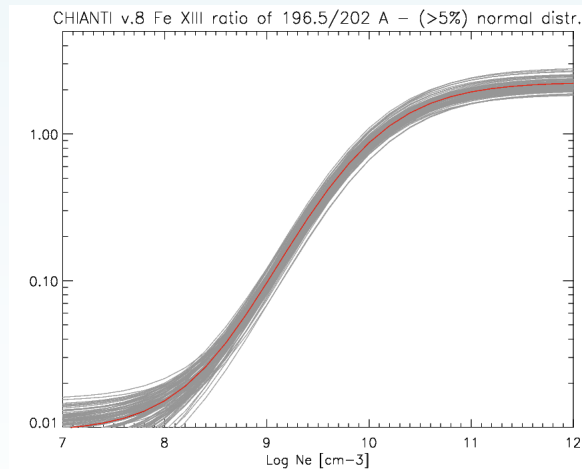


Uncertainties

1) On wavelengths. Each energy level is assessed carefully in CHIANTI. We make some mistakes but in general data are far better than NIST.

2) On rates within an ion can be converted into uncertainties in e.g. line ratios (Yu, Del Zanna+2018)

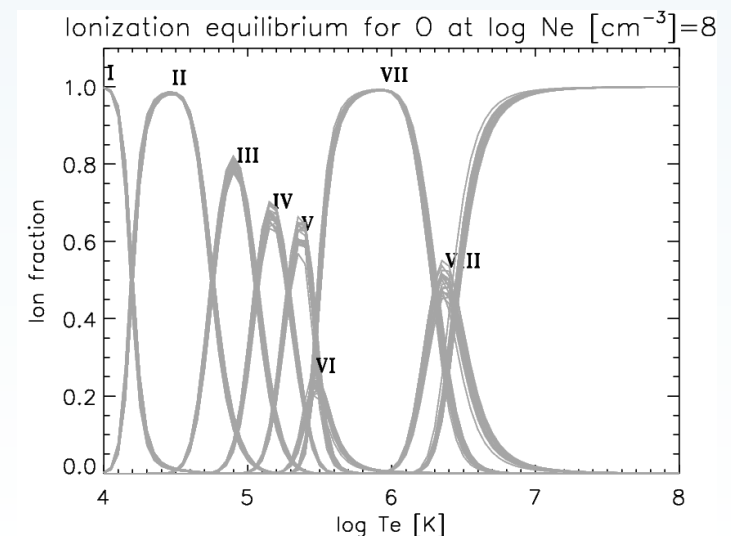
<i>i</i>	Configuration (% purity)	Term	E_{best}	$E_{\text{best}} - E_{\text{NIST}}$
1	$3s^2 3p^5$ (96%)	$2p_{3/2}^o$	0.0 ± 0	0
2	$3s^2 3p^5$ (96%)	$2p_{1/2}^o$	15683.1 ± 1	0
3	$3s 3p^6$ (72%) + 27(c3 24%)	$2S_{1/2}^e$	289236.0 ± 5	-13
4	$3s^2 3p^4$ (3P) 3d(93%)	$4D_{5/2}^e$	388713.5 ± 5	4.5
5	$3s^2 3p^4$ (3P) 3d(94%)	$4D_{7/2}^e$	388708.0 ± 5	-1
6	$3s^2 3p^4$ (3P) 3d(92%)	$4D_{3/2}^e$	390019.0 ± 50	-31
7	$3s^2 3p^4$ (3P) 3d(92%)	$4D_{1/2}^e$	391554.0 ± 50	-1
8	$3s^2 3p^4$ (3P) 3d(92%)	$4F_{9/2}^e$	417652.0 ± 5	-1
9	$3s^2 3p^4$ (1D) 3d(41%) + 29(49%)	$2P_{1/2}^e$	414249.0 ± 500	-
10	$3s^2 3p^4$ (3P) 3d(89%)	$4F_{7/2}^e$	422785.0 ± 10	-10
11	$3s^2 3p^4$ (3P) 3d(95%)	$4F_{5/2}^e$	426260.0 ± 500	-503
12	$3s^2 3p^4$ (3P) 3d(86%)	$4F_{3/2}^e$	427604.0 ± 500	-694
13	$3s^2 3p^4$ (1D) 3d(50%) + 28(38%)	$2P_{3/2}^e$	422844.0 ± 500	-9084
14	$3s^2 3p^4$ (3P) 3d(95%)	$4P_{1/2}^e$	433526.0 ± 500	-1274
15	$3s^2 3p^4$ (1D) 3d(28%) + 31(26%) + 25(25%)	$2D_{3/2}^e$	433088.0 ± 500	-1526
16	$3s^2 3p^4$ (3P) 3d(83%)	$4P_{3/2}^e$	438168.0 ± 500	-



3) On measured ionization and DR rates can be converted into uncertainties in ion charge states

Del Zanna G. - Maui, Jun 2018

Fe X, Del Zanna+2004



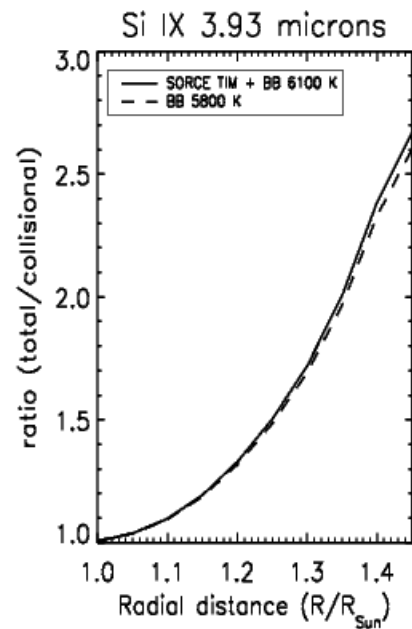
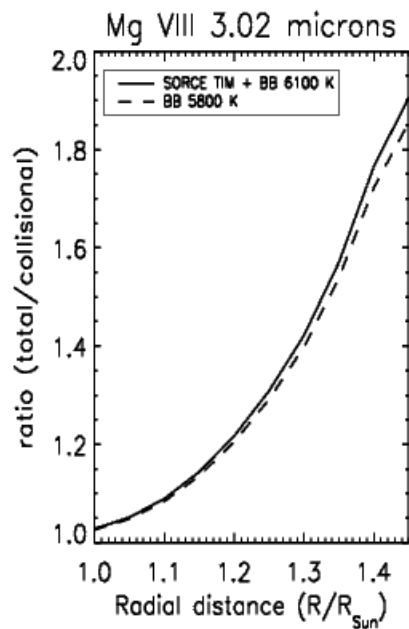
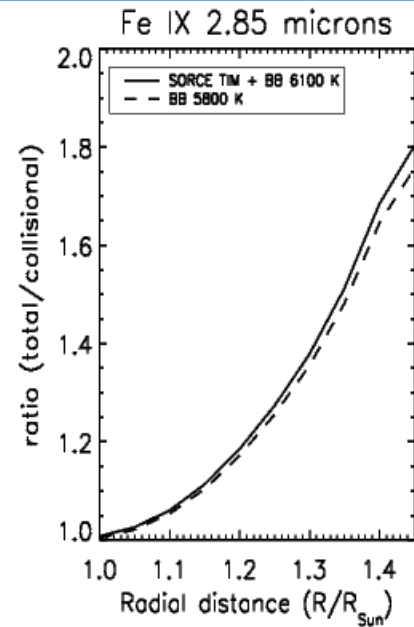
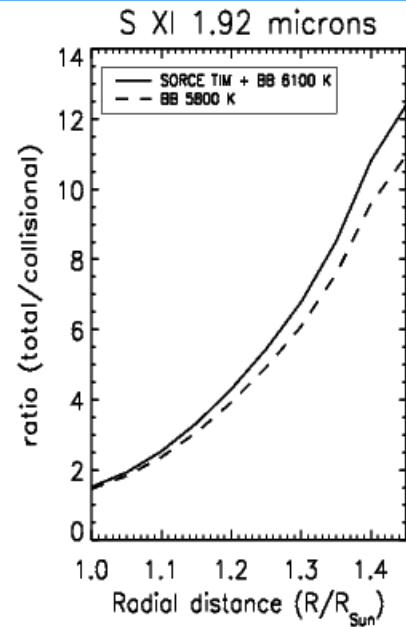
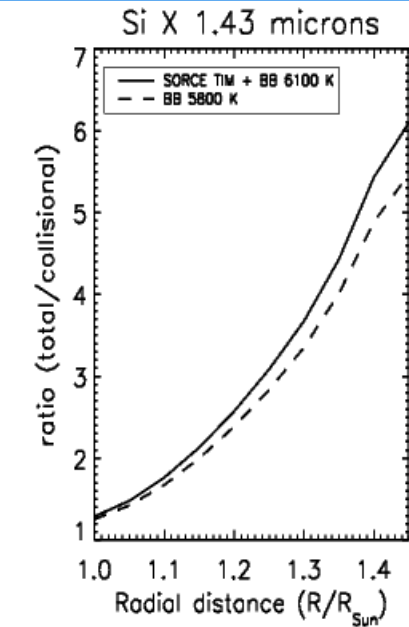
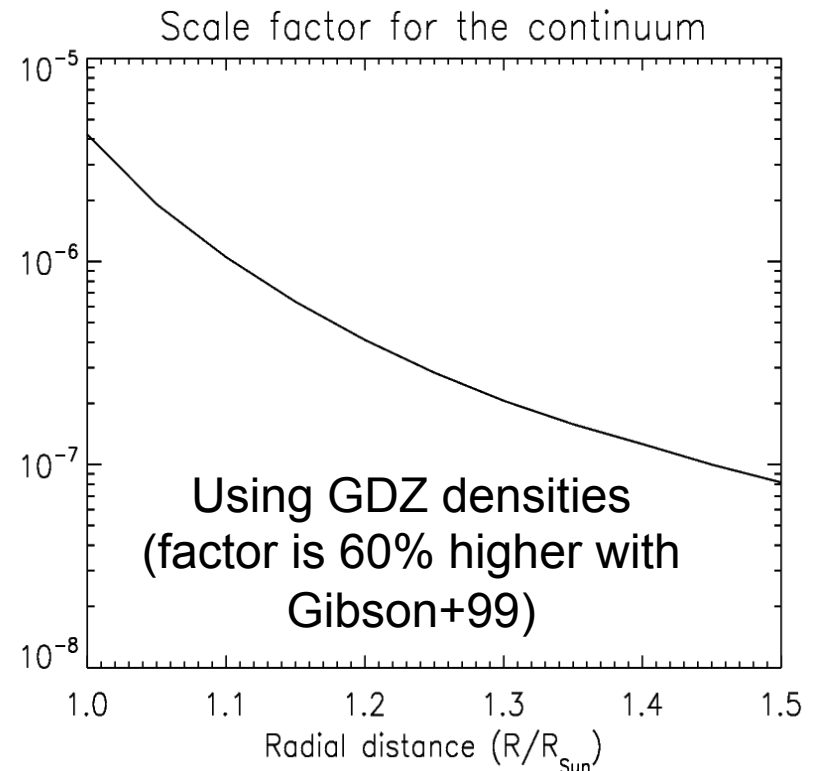
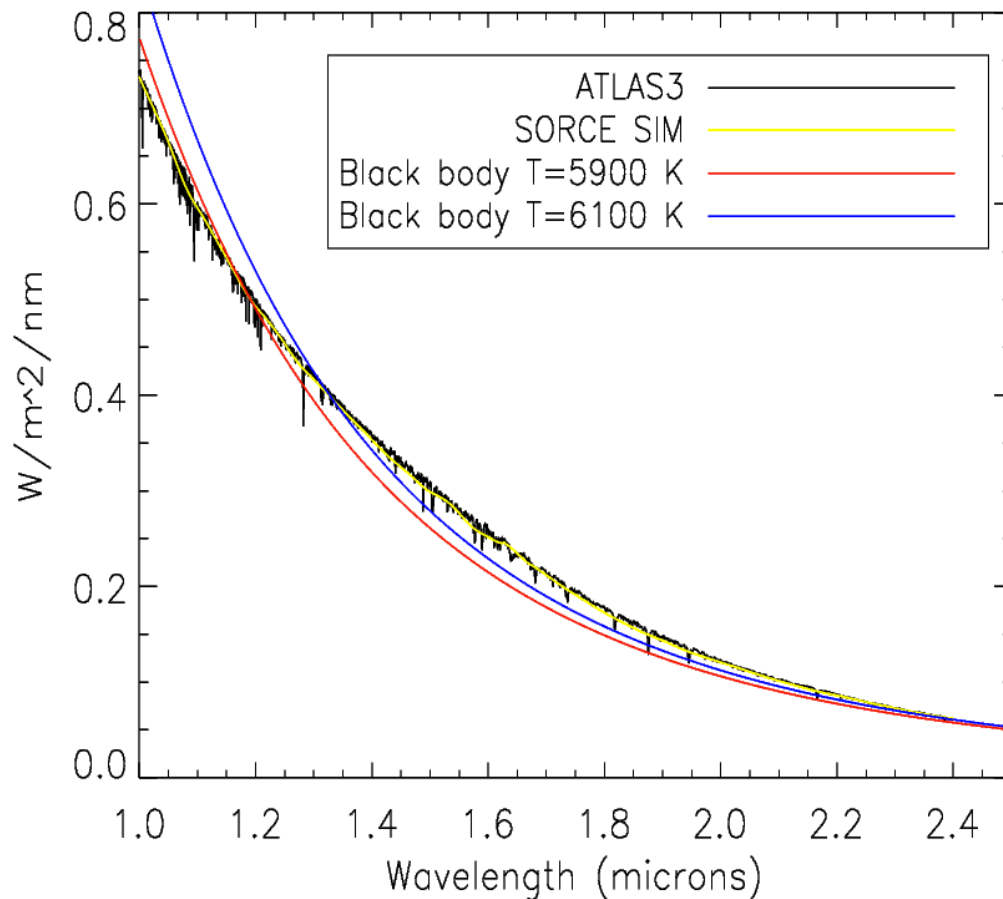


Photo-excitation is significant even in the near-IR. Each spectral line is sensitive to Ne and disk radiation in a different way.

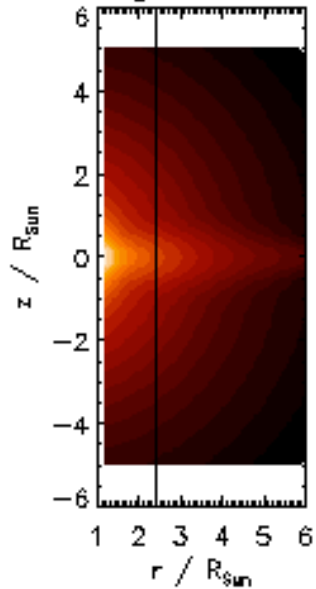
IR continuum – photo-pumping and observed



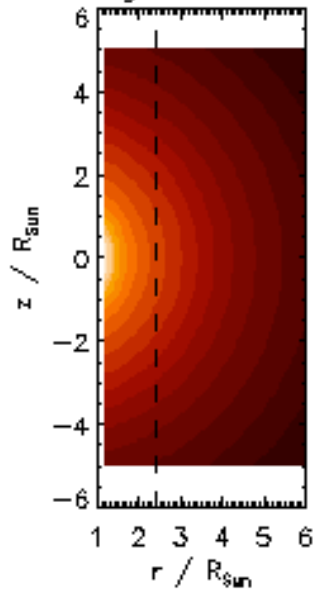
Note: differences between observed and black body.
Missing high-res data above 2.4? (there are observations - Samra).
Even black body should be fine here.
Good news: on the basis of SORCE SIM up to 2.4 microns, no obvious changes
with solar cycle.

Non-trivial issues on N_e , T_e/T_{ionis} distributions

Inhomogeneous density

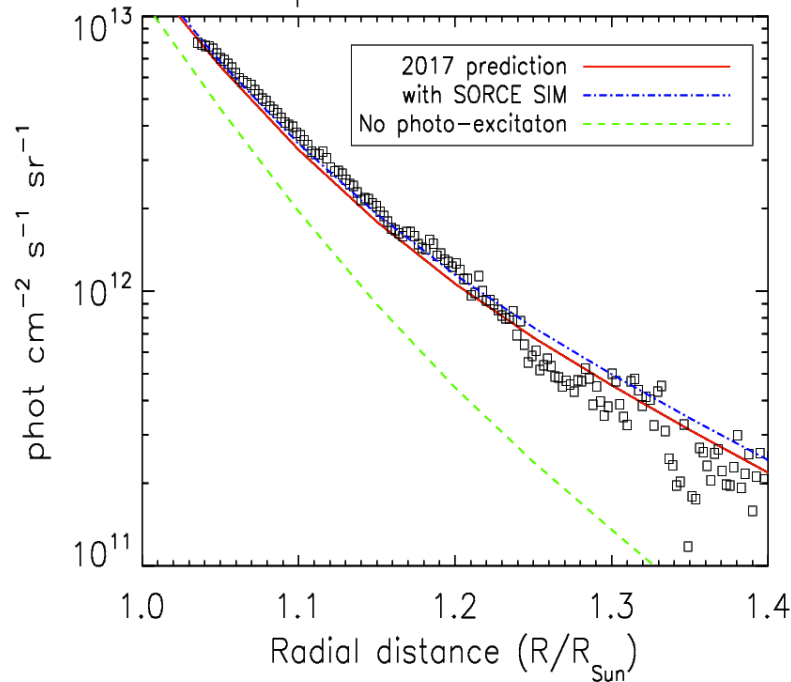


Homogeneous density

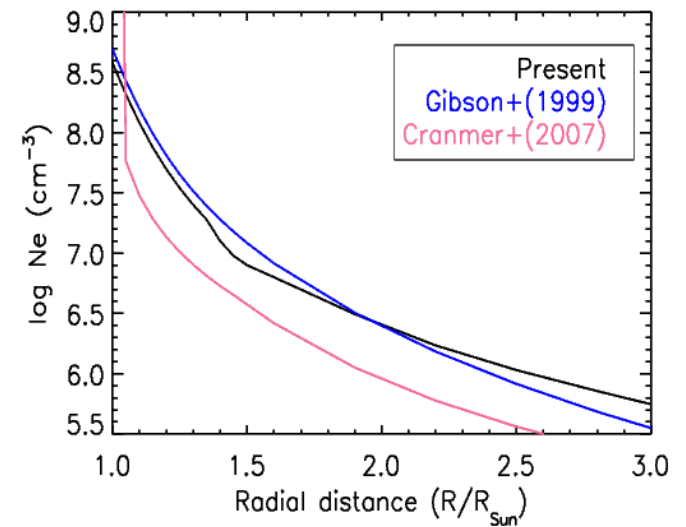
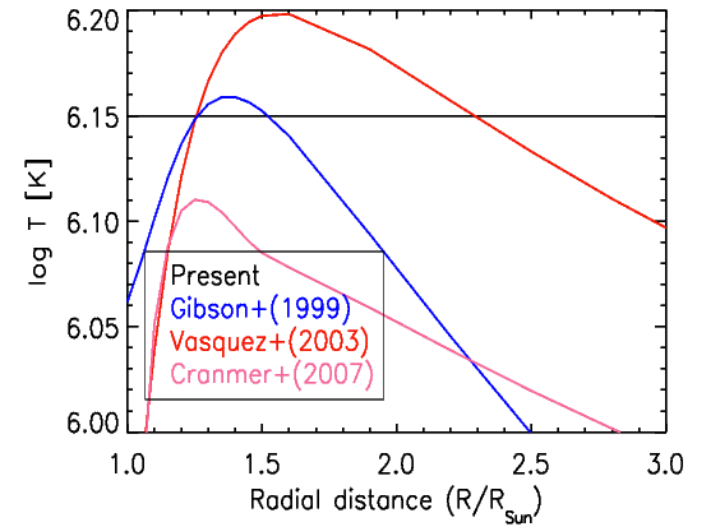
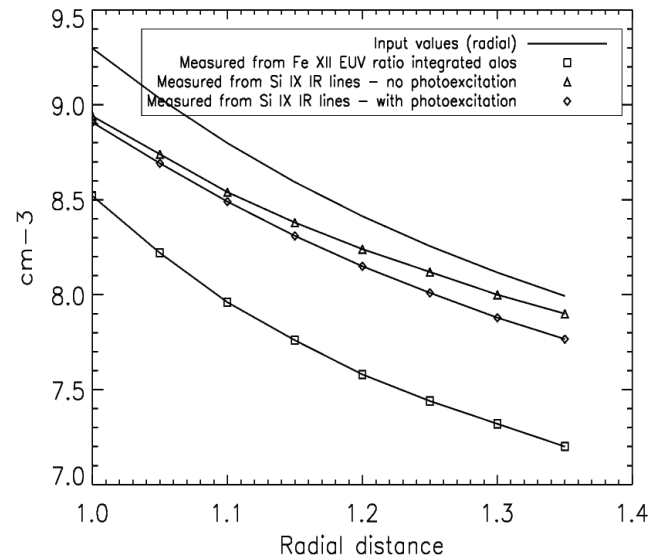


Del Zanna G.

AIR-Spec Si X 1.43 microns



Electron densities



Del Zanna+2018
submitted

Conclusions

- There is a great potential in the forbidden lines but accurate modelling is required.
- New measurements of chemical abundances and densities at high resolution are possible with DKIST
- Synergy with Solar Orbiter.